SCIENTIFIC REPORTS

OPEN

SUBJECT AREAS:
CHEMICAL PHYSICS
BATTERIES
GRAPHENE

Received
11 September 2014

Accepted
21 November 2014

Published
10 December 2014

Correspondence and requests for materials should be addressed to D.L. (dongwookleedl324@gmail.com) or J.S. (jiwonseo606@gmail.com)

Three-dimensionally networked graphene hydroxide with giant pores and its application in supercapacitors

Dongwook Lee[1,2] & Jiwon Seo[3,4]

[1]Department of Physics, Cavendish laboratory, JJ Thompson Avenue, Cambridge, CB3 0HE UK, [2]Division of Physics and Applied Physics, Nanyang Technological University, 637371 Singapore, [3]School of Advanced Materials Science and Engineering, Sungkyunkwan University, Suwon, 440–746 Republic of Korea, [4]Department of Physics and IPAP, Yonsei University, Seoul 120–749, Republic of Korea.

The three-dimensionally networked and layered structure of graphene hydroxide (GH) was investigated. After lengthy immersion in a NaOH solution, most of the epoxy groups in the graphene oxide were destroyed, and more hydroxyl groups were generated, transforming the graphene oxide into graphene hydroxide. Additionally, benzoic acid groups were formed, and the ether groups link the neighboring layers, creating a near-3D structure in the GH. To utilize these unique structural features, electrodes with large pores for use in supercapacitors were fabricated using thermal reduction in vacuum. The reduced GH maintained its layered structure and developed a lot of large of pores between/inside the layers. The GH electrodes exhibited high gravimetric as well as high volumetric capacitance.

Following the discovery of graphene, interest in its superb properties has sparked a great deal of pure and applied research on graphene and graphene-based materials[1–4]. Among the graphene-based materials, graphene oxide (GO)[5–6] is considered an outstanding candidate for a precursor in the preparation of graphene devices since reduced GO has similar properties to graphene[7]. GO is composed of a mixture of two different types of regions: oxidized non-graphitic regions and non-reacted graphitic regions[5–6,8]. The co-existence of these regions produces new properties such as tunable excitons[9–10]. The chemical vulnerability of epoxy groups in GO leads to an increase in the fraction of non-graphitic regions during reaction with NaOH, which destroys most epoxy groups in GO[10]. GO disperses well in dilute NaOH solutions, where the GO layers are exfoliated[11]. Lengthy immersion in a NaOH solution followed by vacuum drying produces graphene hydroxide (GH)[10], which exhibits exotic properties such as a positive temperature coefficient of resistance and a large electron–acoustic phonon coupling constant[10,12]. In addition, half of the carbon atoms in GH have sp^3-hybridized orbitals in a layered structure, which is different from typical graphene-based compounds[10]. A high ratio of sp^3:sp^2 carbon atoms and other structural features, including chemical groups on its surface, give GH a great deal of surface area; this not only enhances its chemical reactivity but also opens up the opportunity for applications in electrodes for supercapacitors and sensors. Therefore, research on the structure of GH would shed light on certain aspects of graphene systems with chemical groups, as well as help realize high–gravimetric-capacitance electrodes for energy storage systems. Here, we report on our investigation of the structure of GH, which is significantly different from that of GO. We found that the 3D structure of GH gives it unique properties. We also report that electrodes for supercapacitors made of reduced GH demonstrate high gravimetric, as well as volumetric, capacitance, and that these properties are related to the 3D structure of GH.

Results

Figure 1 shows optical and SEM images of the GO, NaOH-treated GO (NaOH-GO), and GH paper materials. The GO product was a brown powder [Fig. 1(a)] that turned black after reaction with NaOH [Fig. 1(b)]. Immersion of GO in NaOH for 2 weeks produced GH [Fig. 1(c)]. The SEM images show that microstructure of the GO changed after the reaction with NaOH [Figs. 1(d)–1(f)]. Although the reaction with NaOH made the layers of GO more distinct, the flaky morphology disappeared after long immersion into NaOH-solution [Fig. 1(f)]. Figure 2 shows SEM images of the cross-sections of the GH paper sample of Fig. 1(c). The GH layers were stacked densely, and this layered structure is clearly visible in Figs. 2(e) and (f). Since GH has a layered structure and so many wrinkles, it has a larger surface area than GO.

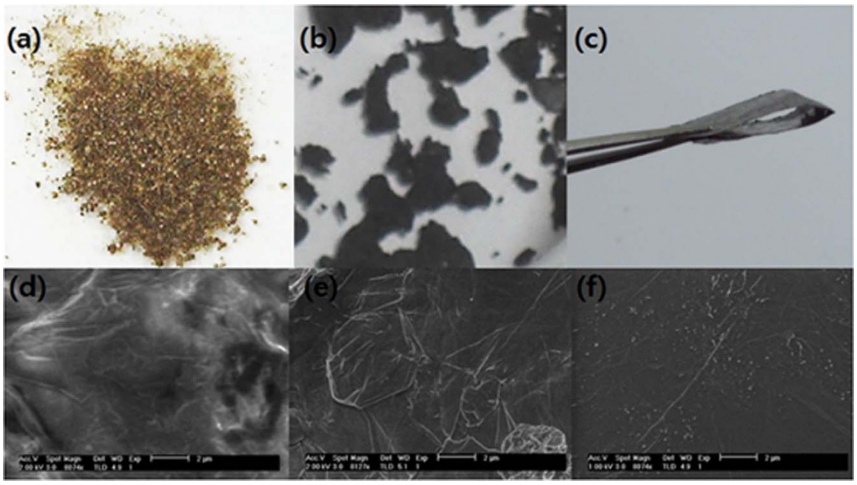

Figure 1 | Optical and SEM images of GO. [(a), (d)] GO, [(b), (e)] NaOH-treated GO, [(c), (f)] GH. The GO initially has a brown color (a) and turns black after epoxy groups were destroyed by NaOH (b). GH paper was prepared by vacuum filtration of NaOH-GO; it looks a flexible film (c).

The structural changes in the GO samples are illustrated in Figure 3. The interlayer spacing (*d*) of GO, inferred from the peak at $2\theta = 12.48^\circ$, was ≈7.1 Å, and the mean crystallite size was 101.6 Å, according to Scherrer formula[14]. After the reaction with NaOH, many tiny sharp peaks arose in the XRD pattern. A broad envelope peak, which is characteristic of an amorphous phase, appeared around 30°, indicating that the structure of GO changed after the destruction of the epoxy groups and that the NaOH-GO was partially amorphous. The peaks below 12° in the NaOH-GO pattern revealed that the interlayer distances in some regions increase to more than 7 Å. The multiple distinct peaks present in the XRD pattern of the NaOH-GO disappeared after lengthy immersion in the NaOH solution, leaving two main peaks at 12.27° and 21.03°. The interlayer distances associated with these are 7.21 Å and 4.22 Å, respectively. Additionally, the broad envelope peak at 30° persisted. The XRD data demonstrated that the GH was different from the GO and even the NaOH-GO. Moreover, the disappearance of tiny sharp peaks of the NaOH-GO pattern reveals that most of the crystalline regions of the NaOH-GO were destroyed. The number of stacked sheets (NS) in the graphene-based materials is given in Table 1; these were obtained by dividing the mean crystallite size by the interlayer spacing[14]. NS decreased after reaction with NaOH, implying that the destruction of epoxy groups led to an increase in the interlayer spacing and a weakening of the bonding between layers. However, the NS value of the GH was larger than those of the other materials, indicating that the layers are more strongly stacked.

The XPS spectra in Fig. 4 illustrate that the GO is composed of two kinds of carbon orbitals. After reaction with NaOH, more carbon atoms had sp^3 orbitals, although most of the carbon atoms in GO have sp^2 orbitals. All of the spectra were decomposed into three components, given in Table 2: sp^2 carbon around 284 eV, C–O bonded carbon at 286 eV, and an additional carboxyl group (C(O)O) near 289 eV[15]. The ratio of carbon sp^2:sp^3 orbitals in the samples were extracted from the XPS spectra. GH had the lowest sp^2:sp^3 ratio of all of the samples.

The chemical groups in the samples were identified using the FT-IR spectra in Fig. 5. The GO sample showed four main peaks centered at 1050, 1380, 1680 and 3470 cm^{-1}. The peak at 1050 cm^{-1} was related to the presence of epoxy groups. The peak observed at 1380 cm^{-1} was assigned to a C–O vibrational mode. The peak at 1680 cm^{-1} corresponded to the vibrational mode of the ketone groups which can be located only on the edge, so it was influenced by the edge conditions such as the shape and the presence of dangling bonds. The peak at 3470 cm^{-1} indicated C–OH stretching. The schematic structure of GO is shown in Figure 6(a).

The number of epoxy groups in GO (1050 cm^{-1}) decreased after the reaction with NaOH, which can decompose the epoxy (–O–) groups into hydroxyl (–OH) groups and –ONa groups. The peak at 1480 cm^{-1} was assigned to C–H (in-plane bending), and the sharp shoulder peak at 905 cm^{-1} was from C–H (out-of-plane bending mode)[16]. In addition, the NaOH-GO showed a shoulder around 3000 cm^{-1}, implying that C–H stretching modes (sp^3) are present in the sample. Moreover, the peaks at 3000 cm^{-1} and 1480 cm^{-1} likely came from hexane groups and are strong evidence that cyclohexane groups were synthesized. The shift of the broad peak around 3400 cm^{-1} toward 3000 cm^{-1} and the sharp peak at 1480 cm^{-1} were

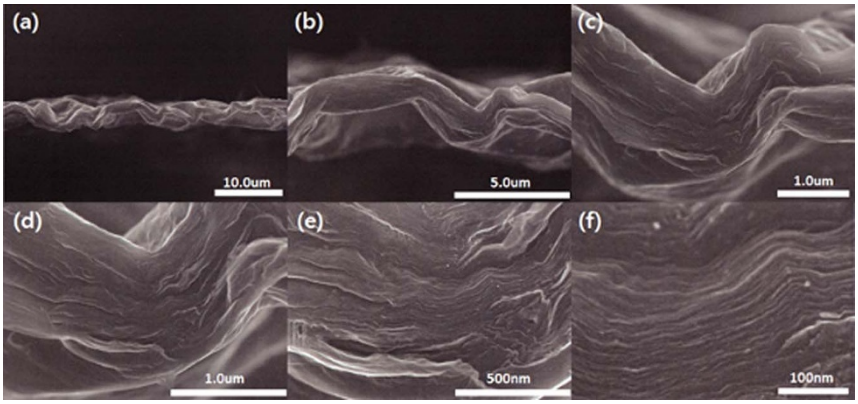

Figure 2 | SEM images of the GH. Cross-sectional SEM images of the GH paper sample at various magnifications.

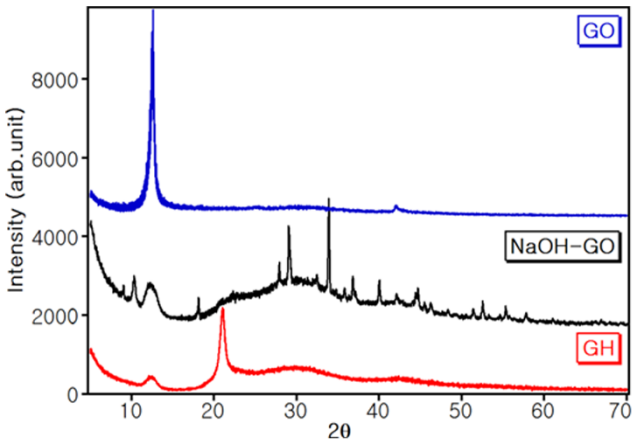

Figure 3 | XRD spectra of the samples. XRD patterns were recorded on a Bruker D8 Advance powder diffractometer with Cu Kα radiation and a step size of 0.02°.

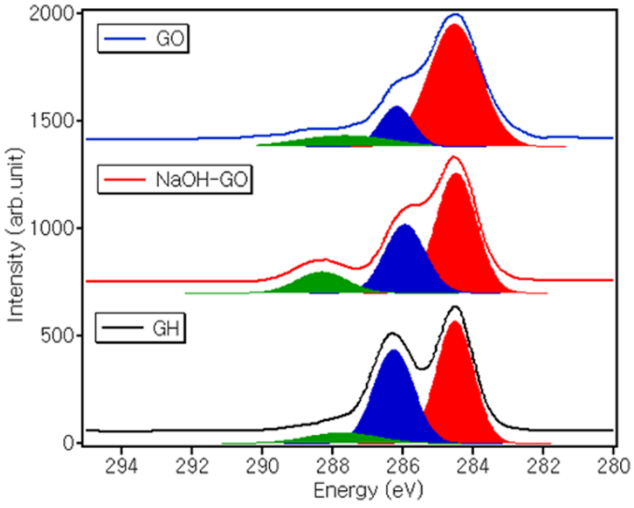

Figure 4 | XPS spectra of the samples. GO (top), NaOH-GO (middle), and GH (bottom).

likely due to the formation of phenol[17], which was confirmed by nuclear magnetic resonance results as well as the FT-IR spectrum of hydrated GO[17]. The schematic of NaOH-GO is displayed in Fig. 6(b).

GH showed a broad peak from the hydroxyl groups at 3400 cm^{-1} and also exhibited a broad peak at 1400 cm^{-1}. The peak at 1600 cm^{-1} was assigned to ketone groups. However, the small peak at 1600 cm^{-1} present in NaOH-GO grew larger. The peak at 1480 cm^{-1} moved to a shorter wavelength of about 1400 cm^{-1}. The two peaks at 1700 cm^{-1} and at 1400 cm^{-1} are common in benzoic acid, rather than carboxyl groups. Thus, the peak at 1700 cm^{-1} likely came from the –C=O in benzoic acid[16,18], whose presence was also confirmed by broad peak at 1400 cm^{-1} because symmetric COO stretching in Na-benzoic acid appears around 1400 cm^{-1}[16]. Long-duration immersion in NaOH solution might cause the formation of benzoic GO. In addition, the peak at 1600 cm^{-1} implied the formation of ether groups as well as ketone groups. The structural model for GH is illustrated in Fig. 6(c). The ether groups might link two neighboring layers and produce the sample's 3D structure. As indicated in Table 1, the number of sheets in GH increases from 18 to 37, implying that layers of the GH were thicker than those of the NaOH-GO.

In our previous study[12], the electron–acoustic phonon coupling constant of GH was determined to be very high and was the dominant factor in the ultrafast dynamics in the material, implying that the acoustic phonon mode was enhanced enormously by the addition of chemical groups, including –OH groups. The 3D structure of GH enhances the vibrational coupling between neighboring layers, leading to strong coupling of electrons and acoustic phonons and a higher dielectric constant[10]. The temperature, as well as the frequency, dependence of the dielectric constant was explained by the existence of functional groups between neighboring layers; since functional groups containing hydroxyl groups are expected to be present between layers, their behavior might be influenced by the frequency, leading to resonant behavior at high frequency. Furthermore, investigation of the structure and properties of GH would help determine pathways for synthesizing graphene since increasing the ratio of sp^3/sp^2 drives the GH system towards a more graphane-like state in which all carbon atoms have sp^3 orbitals. Moreover, these investigations will also facilitate the development of applications, such as sensors and energy storage systems, which exploit the large surface area of these materials.

As a demonstration of a possible application, electrodes for supercapacitors were fabricated using reduced GH. Figure 7 shows the XRD pattern of reduced GH, which contained 3 distinct peaks. The interlayer distances for the planes associated with these peaks were 12.7 Å, 3.43 Å, and 2.96 Å, respectively. After reduction, the reduced GH had a greater interlayer distance than the unreduced GH (cf. Figure 3).

Figure 8 shows images of the cross-sections of thermally reduced GH samples. Since the GH had numerous chemical groups on the surface, gases were generated during the reduction process by the destruction chemical groups such as epoxy and hydroxyl groups. In addition, the vacuum environment triggered the expansion of the stacked layers so that the evolved gases could escape from the GH. Long-term vacuum reduction at high temperature produced many pores inside the sample and expanded the interlayer spacing, i.e., the effective surface area was greatly increased. Therefore, neighboring layers were separated from each other and many pores were clearly visible, as shown in Fig. 8(a). In Figs. 8(b) and (c), the empty space between layers is distinct, and the structure is like that of a connected cocoon. The size of the cocoon-shaped pores was larger than 1 μm^2. Inside the individual layers, there were smaller pores around 250 nm × 50 nm and 40 nm × 10 nm, as shown in Figs. 8(e) and (f), respectively. The sheet resistance of the reduced-GH electrodes was measured using the four-point–probe method and was 1.8 Ω/□.

To evaluate the supercapacitive performance of the reduced GH electrodes, two-electrode symmetric coin cells were assembled. The mass of the GH electrode is 0.198 mg each. To operate the coin cells

Table 1 | Principal structural characteristics obtained from the XRD data in Figure 3

	2θ (°)	*d* (Å)	Mean crystallite size (Å)	NS
GO	12.48	7.09	101.6	28.7
NaOH-GO	12.27	7.21	64.8	18.0
GH	12.27	7.21	133.5	37.0

Table 2 | XPS peak analysis of the data in Figure 4

	284–285 eV (C=C)	286–287 eV (C–O)	288–289 eV (C–(O)–O)	
	Area (%)			sp^2:sp^3
GO	72.7	15.3	12.0	2.66:1
NaOH-GO	55.8	31.9	12.3	1.26:1
GH	50.1	41.5	8.4	1.04:1

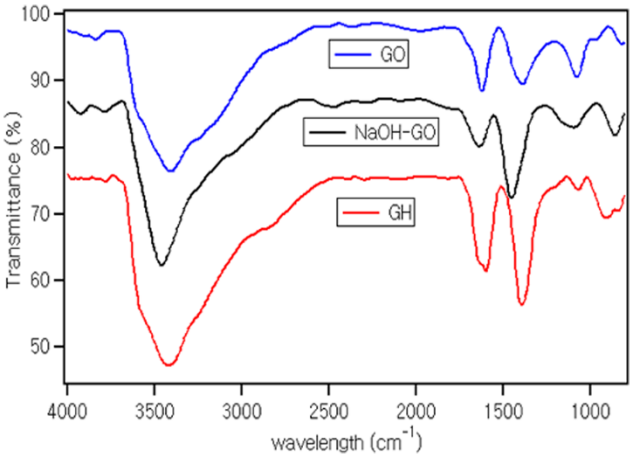

Figure 5 | FT-IR spectra of the samples. GO (top), NaOH-GO (middle), and GH (bottom).

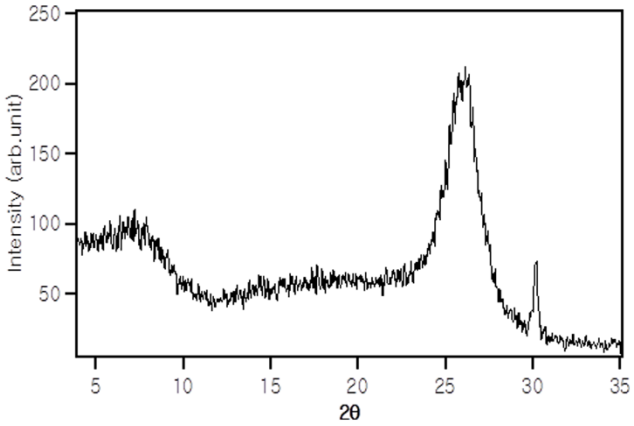

Figure 7 | XRD pattern of reduced GH. The reduced GH had a greater interlayer distance than the unreduced GH.

across a wide voltage range, organic 1 M tetraethyl ammonium tetrafluoroborate (TEABF4) in polycarbonate was used as the electrolyte. The electrochemical performance was analyzed using galvanostatic charge/discharge profiling, cyclic voltammetry (CV), and impedance measurements.

The charge/discharge profiles of the reduced GH electrodes at different current densities are shown in Figure 9. The triangular profiles were similar to those obtained from electrical double-layer capacitors (EDLCs) with good performance. A voltage drop in the curve, caused by an equivalent series resistance, was almost negligible. The specific capacitance (C) of the electrode was calculated using the slope of the discharge line using

$$C = It/m\Delta V, \quad (1)$$

where I is the applied current, m is the mass of active material, ΔV is the potential range, and t is the time to discharge. The specific capacitances of the electrode were 210.1 F/g (at 1 A/g) and 212.3 F/g (at 2 A/g). The volumetric capacitance of each electrode was calculated to be 71.4 F/cm3 and 72.1 F/cm3. The average electrode density was 0.34 g/cm3.

The reduced-GH electrodes showed rectangular CV curves [Fig. 9(b)] without any redox peaks, indicating ideal capacitive behavior. The pseudo-capacitance effect, which can be enhanced by surface functional groups containing oxygen and nitrogen by an additional Faradaic reaction, was not observed. It should be also noted that the CV curves were still rectangular at a high scan rate of 0.1 V/s, indicating rapid charging/discharging with a low equivalent series resistance in the electrodes.

Figure 9(c) displays the electrochemical impedance spectrum of the reduced-GH electrodes. The impedance measurements were carried out at a DC bias of 0 V over a frequency range of 100 kHz to 1 mHz. The impedance curve in Fig. 9(c) is a straight line, indicating ideal capacitive behavior in the device. The intercept of the Nyquist curve with the x axis is about 3.5 Ω, demonstrating the good conductivity of the electrolyte and the very low internal resistance of the electrode.

The intrinsic capacitance of single layer graphene is 21 μF/cm^2[19], which is equivalent to 550 F/g. Previous research has focused on achieving high gravimetric capacitance in graphene and graphene-related materials through the use of porous materials with small densities to achieve supercapacitors with large gravimetric capacitances. However, the porosity of carbonaceous materials (such as graphene foam and graphene hydrogel) negatively impacts the volumetric capacitance of supercapacitors due to low densities (0.01–0.03 g/cm^3)[20–23], which is the greatest barrier to commercialization of supercapacitors requiring large volumetric capacitance for compact energy storage systems. However, the GH electrodes show not only high gravimetric as well as volumetric capacitances, which pave the commercialization path of supercapacitors.

Discussion

We investigated the structure of GH to assess its suitability for use in graphene-based applications. We determined that GH has a layered structure and that, after reduction under high-vacuum and high-temperature conditions, many large pores between the layers developed, leading to high surface area. To utilize this high surface area, electrodes for supercapacitors were manufactured from reduced GH. The layered structure of the reduced GH provided a large volumetric capacitance of 71.4 F/cm^3, as well as a large gravimetric capacitance of 210.1 F/g. Thus, the material investigated here can be used not only for energy storage systems demanding high volumetric capacitance but also accelerate the development of new electric double-layer capacitor (EDLC) materials for supercapacitors with high volumetric capacitance.

Materials

GO samples were prepared by the Brodie process[13]. GO was immersed in a 1 M NaOH solution for 2 weeks. The dispersed GO

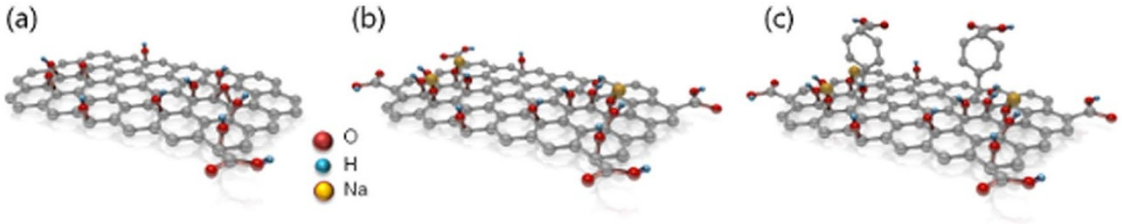

Figure 6 | Schematic structures of the samples. (a) GO, (b) NaOH-treated GO, and (c) GH.

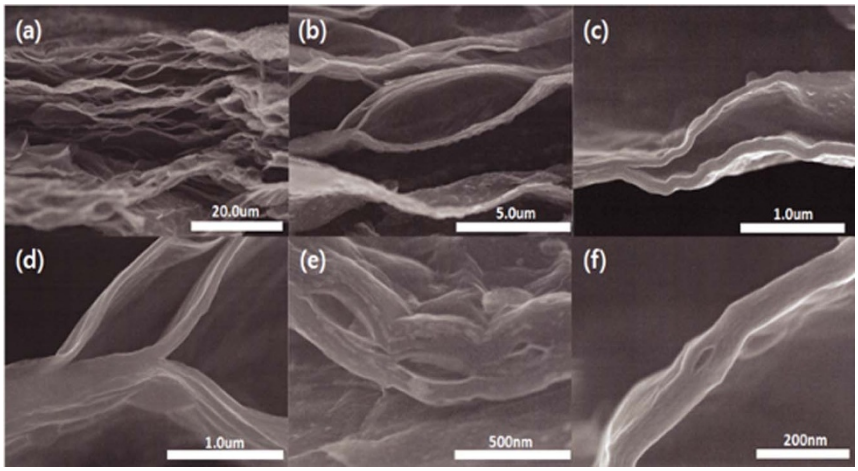

Figure 8 | SEM images of thermally reduced GH. Cross-sectional SEM images of the reduced GH paper sample at various magnifications.

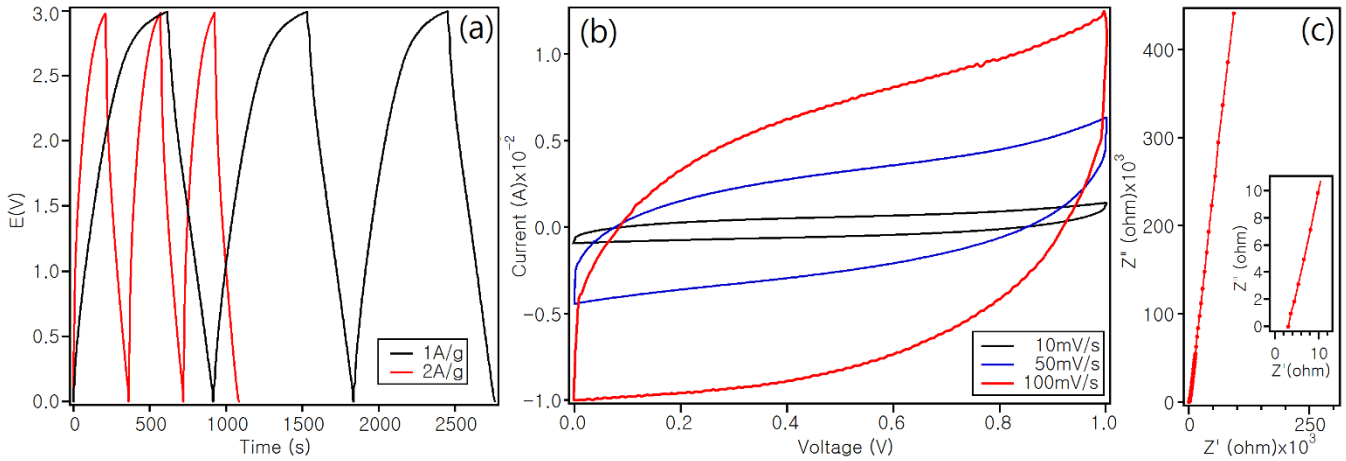

Figure 9 | Electrochemical performance of the reduced-GH electrode. (a) galvanostatic charge and discharge curves at different current densities, (b) *C-V* profiles at different scan rates, and (c) the complex impedance spectrum.

in the NaOH solution was washed with DI water, and GH paper was prepared by vacuum filtration through an anodized aluminum oxide (AAO) filter (47 mm diameter, 200 nm pore size) for a week. The GH samples were prepared by thermal reduction in a vacuum chamber (~1 mTorr) at 800°C for 24 h. The electrodes (12 mm in diameter) were punched out from the as-made reduced film. Two-electrode symmetric coin cells (CR 2032) were assembled. Organic 1 M tetraethyl ammonium tetrafluoroborate (TEABF4) in polycarbonate (PC) was used as the electrolyte.

Characterization

The morphologies of the samples were characterized using a FEI Philips XL30 sFEG scanning electron microscope (SEM). To characterize the structure of the samples, we used a Bruker D8 Advance powder X-ray diffractometer (XRD) with Cu Kα radiation and a step size of 0.02°, a Perkin-Elmer Fourier transform infrared spectrometer (FT-IR), and a Physical Electronics Quantum 2000 X-ray photoemission spectrometer (XPS). Galvanostatic charge-discharge, cyclic voltammetry (CV) and impedance spectroscopy were carried out using a potentiostat (Solartron 1470E). Impedance spectroscopy was carried out in the frequency range of 100 kHz to 1 mHz (Solartron 1470E).

1. Novoselov, K. S. *et al.* Electric field effect in atomically thin carbon films. *Science* **306**, 666–669 (2004).
2. Gundra, K. & Shukla, A. Theory of the electro-optical properties of graphene nanoribbons. *Phys. Rev. B* **83**, 075413 (2011).
3. Osella, S. *et al.* Graphene nanoribbons as low band gap donor materials for organic photovoltaics: quantum chemical aided design. *ACS Nano* **6**, 5539–5548 (2012).
4. Liu, L. *et al.* Graphene oxidation: thickness-dependent etching and strong chemical doping. *Nano Lett.* **8**, 1965–1970 (2008).
5. Lerf, A., He, H., Forster, M. & Klinowski, J. Structure of Graphite Oxide Revisited. *J. Phys. Chem. B* **102**, 4477 (1998).
6. Lee, D. W. *et al.* The Structure of Graphite Oxide: Investigation of Its Surface Chemical Groups. *J. Phys. Chem. B* **114**, 5723–5728 (2010).
7. Stankovich, S. *et al.* Synthesis of graphene-based nanosheets via chemical reduction of exfoliated graphite oxide. *Carbon* **45**, 1558–65 (2007).
8. Lee, D. W. & Seo, J. W. sp^2/sp^3 Carbon Ratio in Graphite Oxide with Different Preparation Times. *J. Phys. Chem. C* **115**, 2705–2708 (2011).
9. Lee, D. *et al.* Quantum confinement-induced tunable exciton states in graphene oxide. *Sci. Rep.* **3**, 1–5 (2013).
10. Lee, D. W. *et al.* Transparent and flexible polymerized graphite oxide thin film with frequency-dependent dielectric constant. *Appl. Phys. Lett.* **95**, 172901 (2009).
11. Rourke, J. P. *et al.* The real graphene oxide revealed: stripping the oxidative debris from the graphene-like sheets. *Angew. Chem.* **123**, 3231–3235 (2011).
12. Lee, D. *et al.* Ultrafast carrier phonon dynamics in NaOH-reacted graphite oxide film. *Appl. Phys. Lett.* **101**, 021604 (2013).
13. Brodie, B. C. On the atomic weight of graphite. *Philos. Trans. R. Soc.* **149**, 249 (1859).
14. Patterson, A. L. The Scherrer Formula for X-Ray Particle Size Determination. *Phys. Rev.* **56**, 978–982 (1939).
15. Pirkle, A. *et al.* The effect of chemical residues on the physical and electrical properties of chemical vapor deposited graphene transferred to SiO_2. *Appl. Phys. Lett.* **99**, 122108 (2011).

16. Ibrahim, M., Nada, A. & Kamal, D. E. Density functional theory and FTIR spectroscopic study of carboxyl group. *Indian J. Pure Appl. Phys.* **44**, 911–917 (2005).
17. Lee, D. W. & Seo, J. W. Formation of Phenol Groups in Hydrated Graphite Oxide. *J. Phys. Chem. C* **115**, 12483–12486 (2011).
18. Le, DuyDuc. The modification of graphene oxide and studies of the detection of norovirus DNA and RNA. Diss. Kansas State University. 2013.
19. Xia, J., Chen, F., Li, J. & Tao, N. Measurement of the quantum capacitance of graphene. *Nat. Nanotechnol.* **4**, 505–509 (2009).
20. Zhang, L. *et al*. Porous 3D graphene-based bulk materials with exceptional high surface area and excellent conductivity for supercapacitors. *Sci. Rep.* **3**, 1408 (2013).
21. Largeot, C. *et al*. Relation between the ion size and pore size for an electric double-layer capacitor. *J. Am. Chem. Soc.* **130**, 2730–2731 (2008).
22. Niu, Z., Chen, J., Hng, H. H., Ma, J. & Chen, X. A. leavening strategy to prepare reduced graphene oxide foams. *Adv. Mater.* **24**, 4144–4150 (2012).
23. Worsley, M. A. *et al*. Synthesis of graphene aerogel with high electrical conductivity. *J. Am. Chem. Soc.* **132**, 14067–14069 (2010).

Acknowledgments

This work was supported by the National Research Foundation of President Post-doctoral fellowship Program (NRF-2013R1A6A3A060443). The authors are grateful to J.J. Richard for the SEM images.

Author contributions

D.L. managed the project, prepared the samples, carried out experiments, wrote the manuscript, and analyzed the data; J.S. wrote the manuscript and analyzed the data. All authors reviewed the manuscript.

Additional information

Competing financial interests: The authors declare no competing financial interests.

How to cite this article: Lee, D. & Seo, J. Three-dimensionally networked graphene hydroxide with giant pores and its application in supercapacitors. *Sci. Rep.* **4**, 7419; DOI:10.1038/srep07419 (2014).